Available online at www.sciencedirect.com
ScienceDirect
Catalysis Communications 9 (2008) 1551–1557
CATALYSIS COMMUNICATIONS
www.elsevier.com/locate/catcom

A study of co-precipitated bimetallic gold catalysts for water–gas shift reaction

María-Asunción Hurtado-Juan [a], Connie M.Y. Yeung [a], Shik Chi Tsang [a,b,*]

[a] The Surface and Catalysis Research Centre, School of Chemistry, University of Reading, Whiteknights, Reading RG6 6AD, UK
[b] Wolfson Catalysis Centre, Inorganic Chemistry Laboratory, University of Oxford, Oxford OX1 3QR, UK

Received 7 August 2007; received in revised form 20 December 2007; accepted 21 December 2007
Available online 11 January 2008

Abstract

Synthesis, testing and characterisation of bimetallic gold, Au–M on ceria as catalysts were carried out for low temperature water–gas shift reaction (WGS). Amongst the entire screened catalysts 3 wt% (Au–Pt)/CeO_2 displayed the best WGS activity than the monometallic promotors, giving the light-off curve at the lowest temperature in the range 100–300 °C. (Au–Pd)/CeO_2 also achieved the same activity but at a higher temperature. It was also found that WGS activity was strongly correlated with the surface reducibility which in turn depended on the modified local electronic band structure of promoted ceria. These results clearly suggest that the key role of bimetallic promoter may involve in facilitating the creation of defective reduced surface by exerting its local electronic effect on ceria to form the surface germinal –OH groups in water which act as active sites for enhanced WGS activity.
© 2008 Elsevier B.V. All rights reserved.

Keywords: Gold; Water–gas shift; Ceria; Bimetallic; TPR; UV–visible reflectance

1. Introduction

Catalysed water–gas shift reaction, WGSR ($CO_{(g)} + H_2O_{(g)} \rightarrow CO_{2(g)} + H_{2(g)}$) is a key step in the generation of clean hydrogen from hydrocarbons that is essential to enable the future hydrogen economy. Recently, there is renewed interest in the WGS reaction due to its potential use is supplying hydrogen for fuel-cell power generations which are undergoing a very fast development for both stationary and mobile applications [1]. A typical fuel-cell choice is a proton exchange membrane (PEM) because it offers a series of advantages like as compactness, low operating temperature, suitability to no continuous operation, and long stack life [2], but it requires hydrogen with a low CO concentration. The purpose of the WGS reaction is thus to convert CO from the reformate gas to CO_2 coupled with the conversion of water to hydrogen. The WGSR is moderately exothermic ($\Delta H^{\circ}_{298} = -41\ kJ\ mol^{-1}$) and hence its equilibrium constant decreases with the temperature, and high conversions are favoured by low temperatures [3].

Catalysts based on cerium oxide are promising for these applications [4–9]. Ceria oxide is classified as an n-type semiconducting oxide with extremely high oxygen mobility where its electronic conductivity and oxygen vacancy can be easily altered by using different promoters and different testing conditions [10]. A number of unique properties associated with ceria have been realised including high redox properties, maintaining high dispersion for metal nanoparticles, hence giving high activity for CO oxidation at low temperature and high WGS activity [11,12]. Amongst the cerium oxide based catalysts studied for WGS, gold promoter has been particularly shown to possess higher activity than other noble metals for the low temperature WGS reaction [8,13].

However, the preparation method has been reported to directly affect the reactivity of the gold–cerium oxide

* Corresponding author. Address: Wolfson Catalysis Centre, Inorganic Chemistry Laboratory, University of Oxford, Oxford OX1 3QR, UK. Tel./fax: +44 1865 282610.
E-mail address: edman.tsang@chem.ox.ac.uk (S.C. Tsang).

1566-7367/$ - see front matter © 2008 Elsevier B.V. All rights reserved.
doi:10.1016/j.catcom.2007.12.026

system. The currently employed methods of impregnation, deposition–precipitation, co-precipitation, and chemical vapour deposition strongly influenced catalytic activity due to the large differences in gold particles size and/or to the availability of active gold sites in close contact with ceria defects on the surface [8,13]. It is also noted that the deposition–precipitation technique was found to be the most promising. Incorporation of other rare-earth elements (i.e. La, Zr) into the ceria is reported to enhance the WGS activity [13]. The active form of the gold on ceria for the WGS reaction is also the subject of much debate. It has been generally thought that metallic gold particles at low dimensions display exceptional catalytic effect. Recently, it has been shown that by stripping the metallic gold particles from the ceria support, the activity of the catalyst is maintained [1]. This result tends to show that the metal in the form of metallic nanoparticles could be inactive and that isolated gold ions are likely to also play an important role in the catalytic process.

In this short paper, co-precipitation technique was employed to prepare a number of bimetallic gold–ceria catalysts which were then tested for low temperature water–gas shift reaction as compared to monometallic gold or noble metal on ceria. As far as we are aware, the use of bimetallic gold as a promoter on ceria by blending another metallic component into gold, has not been systematically studied despite the fact that Venugopal et al. reported their preliminary observation on addition of second metal to gold promoter in the Fe_2O_3 based system [14]. Thus, detailed characterisations of the catalyst samples by temperature programme reduction (TPR) and ultraviolet and visible (UV–visible) diffuse reflectance were made. From this work it is also hoped to shed light on the role(s) of gold or bimetallic promoter on ceria for the low temperature WGS reaction.

2. Experimental

2.1. Catalyst preparation

All the catalysts were prepared using co-precipitation method by mixing solutions of trihydrate chloroauric acid, $HAuCl_4 \cdot 3H_2O$, cerium nitrate hexahydrate, $Ce(NO_3)_3 \cdot 6H_2O$ and M = metal-nitrate except for tungsten (tungsten (IV) carbonyl was used) in a container. Sodium carbonate was then added to the reaction mixture slowly and gradually until the pH of the solution reached 8.0 at 60–70 °C. The precipitate was aged for 90 min in the reaction mixture, centrifugally separated and washed with deionized water until there were no anions detectable in the wash. The materials were then dried overnight at 110 °C and calcined at air at 400 °C for 3 h.

2.2. Catalyst characterisation

X-ray powder diffraction (XRD) analysis of the materials was performed on a Siemens D5000 diffraction system using copper Kα radiation of wavelength 1.54056 Å. The diffractograms were collected from $2\theta = 4$–64° with a 0.050° step size. Identification of the crystalline phases in the material was carried out by comparing the collected diffractogram with the published files from the International Centre of Diffraction Data (JCPDS – 1996). Instrumental peak broadening has been taken into account using $KBr_{(S)}$ as a reference. The average crystalline sizes of the metal and ceria oxide were calculated based on peak broadening using the Debye–Scherrer equation. Elemental analysis of each sample by Energy Dispersive X-ray (EDX) analysis technique was carried by making use of the characteristic X-rays emitted from the sample in Philips CM20 transmission electron microscope. The surface areas of the calcined materials were determined using N_2 (BET) adsorption at −196 °C by commercial equipment, the Sorptometomatic 1990 (CE instruments).

Temperature programmed reduction (TPR) was carried out using a commercial TPR apparatus (TPD/R/O 1110) from ThermoQuest CE Instruments. The samples were first pre-treated with 20 ml min^{-1} of helium during 30 min at room temperature to eliminate possible contaminants. Then 20 ml min^{-1} of 5% H_2 in argon was allowed to pass over 20 mg of sample in a quartz tube. The reactor tube was heated at a rate of 10 °C min^{-1}–1100 °C, and the consumption of hydrogen over the oxide catalyst was monitored by a thermal conductivity detector.

2.3. Catalyst activity measurements

A typical experimental set up for the WGS reaction is as follows: the reactor used for the reactions was a 0.3 m-long quartz tube with internal diameter of 4 mm mounted vertically in a temperature controllable furnace. Fifty milligram of catalyst was packed and sandwiched between two glass wool plugs in the middle of the reactor. The feed gases were then allowed to pass directly through the catalyst bed of the reactor. The furnace temperature was controlled by a temperature controller. A cylinder of CO blended with trace methane as a marker (0.95% CH_4 in 99.05% CO) was used to provide 3 ml min^{-1} of this gas mixture together with 40.5 ml min^{-1} steam flow (0.03 ml min^{-1} liquid water was delivered from a high-performance liquid chromatography pump and then passed through a hot zone at 120 °C in order to generate the steam flow). Thus, the total weight hourly space velocity (WHSV) was set at about 52,000 h^{-1} with the H_2O/CO ratio of 13.5. Under such a high H_2O/CO ratio the water–gas shift equilibrium position tended to lie very much on the forward side, giving nearly complete CO conversions at below 500 °C The sample was pre-treated in the CO/CH_4 gas mixture at a flow of 3 ml min^{-1} at 75 °C for two hours before it was mixed with the steam and tested over a temperature range of 75–500 °C. During testing, at least 60 min was given for the catalyst to reach a stable state at a particular temperature before any measurement of catalytic activity was taken. Three batches of product gas samples were analysed at

each temperature within the 60 min in order to ensure the data as reproducible. The three analyses were generally in agreement with each others hence they were averaged as a single value at the particular temperature. No noticeable catalyst deactivation over all the samples was observed. The methane content in the product gas was also recorded during the catalytic testing in order to assess the degree of methane formation over the particular catalyst.

The product gas mixture was analysed by an online GC using PERKIN ELMER Auto System XL equipped with a methanator and a flame ionisation detector (FID). The size of a sample loop was 1.0 ml. A packed GC column of Carbosphere 80/100 (6 ft × 1/8 in. outer diameter) was used to separate CO, CO_2 and CH_4 from the gas mixture at an oven temperature of 150 °C within five minutes prior to their analysis by the FID. It is noted that a cold trap kept in an ice/water bath at zero degree Celsius was installed between the gas exit of the reactor and the inlet of a gas chromatograph (GC) in order to remove any water from the product mixture otherwise the presence of water would affect the methanator performance of the GC. A second GC (Perkin Elmer XL equipped with TCD detector) was used to check regularly the carbon and hydrogen balances of the exit gas stream for each catalyst before the cold trap at ambient temperature and elevated temperatures which were generally agreed within 95%.

The analogous signal from the GC was converted to digital data using Model 2600 Single Instrument Chromatography Software, which was linked to the GC via a PENELSON 900 Series Interface. The peaks were calibrated to represent their corresponding molar quantities. WGS catalytic activity was expressed in terms of carbon monoxide fraction conversion.

3. Results

3.1. XRD

XRD patterns of ceria with and without doping of gold bimetallic promoters were collected. Fig. 1 shows the typical patterns of pure CeO_2 (upper line) together with some Au–M/CeO_2 catalysts prepared by the co-precipitation technique. The average diameter of the ceria in all our samples is 9 ± 1 nm. This was calculated on the basis of the (1 1 1) peak broadening according to Scherrer's equation (taking account of instrumental broadening). The average size of the typical gold bimetallic promoters is estimated to be ~3 nm with the exceptions of Au/CeO_2 and Au–Ni/CeO_2 samples where a very large size gold particles of ~22 nm is recorded. This is in a sharp contrast to extremely well-dispersed Au/CeO_2 commonly prepared by deposition–precipitation method [13]. It is attributed to the aggregation of gold particles during our co-precipitation and aging treatments over these two samples. On the other hand, it is interesting to find that the incorporation of metallic precursors into gold precursor over the other gold bimetallic samples (i.e. Pd, Pt, W, Ca) clearly result in a good dispersion of gold containing particles on ceria. However, it is not yet known the reason for the phase segregation in the case of Au–Ni/CeO_2 sample.

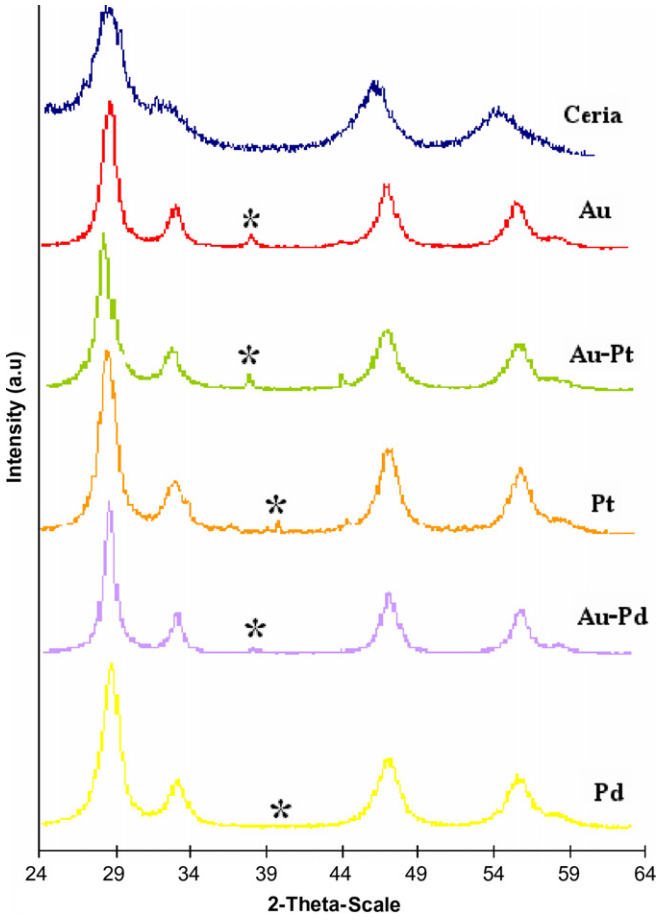

Fig. 1. Typical X-ray powder diffraction patterns of pure CeO_2 (uppermost line), other monometallic and gold bimetallic CeO_2 catalysts prepared by co-precipitation technique. An estimation of ceria particle size via CeO_2 (1 1 1) line broadening from the diffractogram with taking instrumental broadening into account shows the ceria particle size of about 9 ± 1 nm. Metal size is estimated to be ~3 nm but with a large degree of error because of the extremely broad metal or alloy (1 1 1) peak marked with * ($2\theta = \sim 39°$).

3.2. WGS activity evaluation

Water–gas shift activities over these gold bimetallic samples were evaluated and are shown in Fig. 2. With an increase in reaction temperature the WGS activity is generally found to increase for all the catalysts studied. All the gold containing ceria catalysts exhibit a good activity at low temperature range of 150–450 °C despite the fact that a high substrate concentrations and high WHSV used. Different catalysts show very different light-off curves. For example, the Au–Pt/CeO_2 clearly displayed a much higher activity at the same temperature as compared to the Au/CeO_2. The WGS activities over these samples are ranked to be: Au–Pt > Pt > Au–Pd > Au–Ca ⩾ Au–W > Pd > Au–Ni > Au. It is especially noted that the light-off

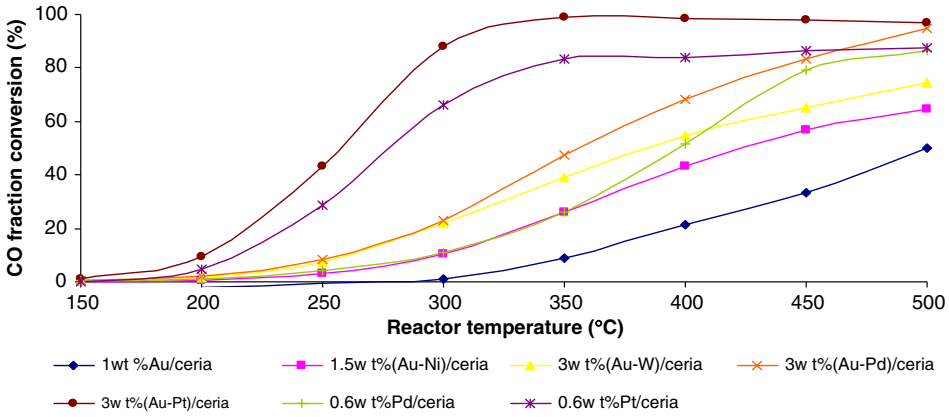

Fig. 2. A plot of CO fraction conversion versus reactor temperature over various Au–M bimetallic promoters on CeO_2.

activities of the bimetallic gold and other metal supported catalysts were directly compared at this stage without using their normalised specific activities (activity per metal site) since the interaction(s) between different metals over these new gold bimetallic catalysts is not clear. However, the total number of the metal sites per gram of catalyst evaluated via CO chemisorption with the assumption of 1:1 CO to metal site ratio is given for comparison (Table 1).

3.3. TPR

TPR Profiles of CeO_2 (a) monometallic and gold bimetallic doped CeO_2 samples: Au–Pt/CeO_2 (b); Au–Pd/CeO_2 (c); Pd/CeO_2 (d); Pt/CeO_2 (e); Au–W/CeO_2 (f); Au–Ca/CeO_2 (g); Au–Ni/CeO_2 (h) and Au/CeO_2 (i) are shown in Fig. 3. As seen from the figure, CeO_2 shows two distinct reduction peaks, one at 440 °C (assigned to reduction of surface oxygen) and a high temperature peak at 800 °C (reduction of bulk ceria oxygen). It is clear that incorporation of ceria with gold bimetallic promoters dramatically facilities reduction of surface oxygen at lower temperatures while the reduction of bulk oxygen remains unchanged. The only exceptions are the Au–Ni/CeO_2 (h) and Au/CeO_2 (i) samples with a very small sized first reduction peak (surface oxygen associated with primary small gold particles) associated with another large surface oxygen reduction peak (with aggregated gold particles which is also reflected by XRD) at higher temperatures (300–400 °C). This clear suggests the preparation technique and additives used strongly influence reduction (and WGS activity) due to difference in gold particle size and to the availability of active gold sites in close contact with ceria defects on the surface. It is also very interesting to reveal from Table 1 that there is nearly a perfect match between the ranked order of first reduction peak (surface oxygen) from lowest temperature to highest temperature (Au–Pt > Pt > Au–Pd > Au–Ca ⩾ Au–W > Pd > Au–Ni > Au) to their ranked order in WGS activity. It clearly implies the degrees of oxygen deficiencies in these gold bimetallic promoted ceria samples must somehow relate to the WGS activity.

3.4. Band structure modification

As stated ceria is n-type of semiconducting oxide the electronic band structure can be modified by promoter(s). From typical diffuse UV reflectance spectra, a clear shift of the absorption edge (O_{2p}–Ce_{4f}) of the ceria upon doping either Au or Au–Pd was observed. The degree of band gap enlargement was clearly found to relate to different bimetallic promoters (see Table 2), the order of which was remarkably similar to both the orders of surface oxygen reducibility and WGS activity. From the data, it suggests that an electron transfer mechanism may take place at

Table 1
The positions of the first (surface oxygen in promoted ceria) and last reduction (bulk oxygen in promoted ceria) peaks from the TPR profiles (refer to Fig. 3)

Catalyst	Metal content (EDX)	Metal sites (μmol g^{-1})	N_2 BET (m^2 g^{-1})	First peak max. (°C)	Last peak max. (°C)
1 wt% Au/CeO_2	1.21 wt% Au	2.778	133.0	~240	~800
1.5 wt% (Au–Ni)/CeO_2	1.08 wt% Au, 0.32 wt% Ni	5.377	114.5	~220	~800
1.5 wt% (Au–Ca)/CeO_2	1.12 wt% Au, 0.20 wt% Ca	n.d.	n.d.	~218	~800
3 wt% (Au–W)/CeO_2	1.10 wt% Au, trace W	3.425	n.d.	~200	~800
0.6 wt% Pd/CeO_2	0.45 wt% Pd	3.710	83.0	~135	~800
0.6 wt% Pt/ CeO_2	0.59 wt% Pt	3.846	85.8	~138	~800
3 wt% (Au–Pd)/CeO_2	1.42 wt% Au, 0.99 wt% Pd	2.507	102.3	~130	~800
3 wt% (Au–Pt)/CeO_2	1.05 wt% Au, 1.75 wt% Pt	2.560	124.3	~120	~800

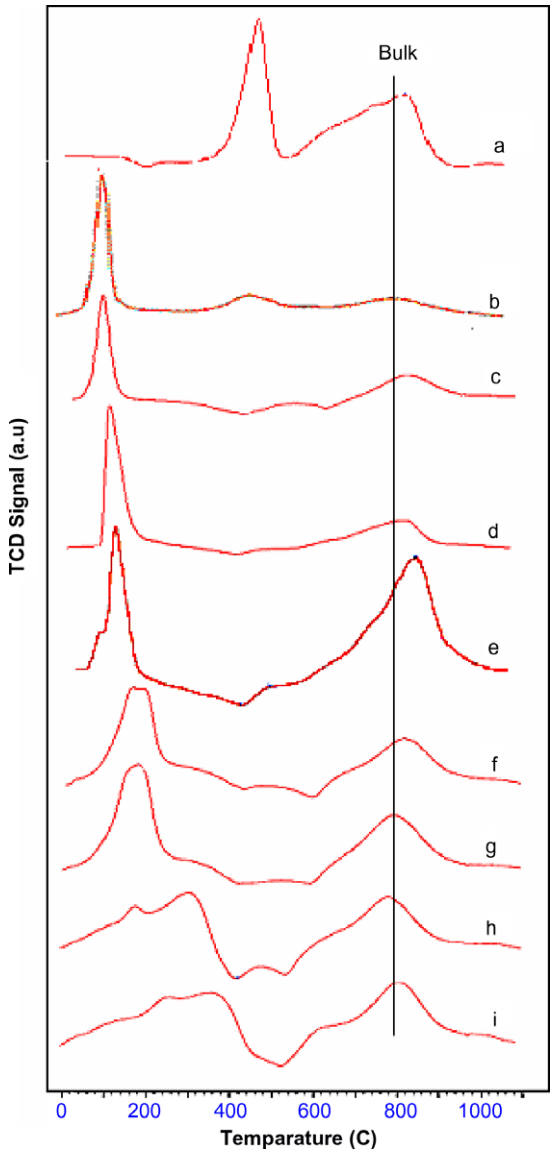

Fig. 3. TPR Profiles of CeO_2 (a) monometallic and gold bimetallic doped CeO_2 samples: Au–Pt/CeO_2 (b); Au–Pd/CeO_2 (c); Pd/CeO_2 (d); Pt/CeO_2 (e); Au–W/CeO_2 (f); Au–Ca/CeO_2 (g); Au–Ni/CeO_2 (h) and Au/CeO_2 (i) which clearly show the significant shift in first reduction peak (surface oxygen in promoted ceria) upon doing with different metal promoters.

the interface between ceria and metallic components (with a higher work function) in facilitating the redox properties of the ceria [10].

4. Discussion

From our results, it is evident that the high WGS activity of Au–M/CeO_2 for the low temperature water–gas shift reaction is apparently related to the nature of surface oxygen in CeO_2 which is easily reduced at low temperatures through the action of the metal particles. It is noted that Hiaire et al. showed that ceria exists in a reduced state under WGS conditions [15]. Amongst the different promoters we studied, Au–Pt appeared to be more effective than

Table 2
The change in band gaps of the electronic transition in different gold doped ceria catalysts (O_{2p}–Ce_{4f}) evaluated by UV–visible diffuse reflectance (refer to Fig. 4)

CATALYST	BAND GAP	
	λ (nm)	(eV)
CeO_2	480	2.582
1 wt% Au/CeO_2	422	2.938
1.5 wt% (Au–Ni)/CeO_2	420	2.952
1.5 wt% (Au–Ca)/CeO_2	415	2.988
3 wt% (Au–W)/CeO_2	412	3.010
3 wt% (Au–Pd)/CeO_2	410	3.024
3 wt% (Au–Pt)/CeO_2	409	3.032

Using the equation: $\alpha(h\upsilon) = A(h\upsilon - E_g)^{m/2}$, where α is the absorption coefficient, $h\upsilon$ is the photon energy, E_g is the direct band gap energy, A is the absorbance of the sample, and $m = 1$ for the direct band transition between bands. Thus, α is zero, then $E_g = h\upsilon = 1240/\lambda$. The absorption wavelength is obtained from the intersection of the graph showing reflectance against wavelength.

Pt, Pd and Au alone on ceria in giving higher WGS activity at lower temperatures The temperatures for its surface oxygen reduction peaks were 120 °C while the reduction peak in the case of Pt and Pd promoters were 130°C and 135 °C, respectively. It is noted that Fu et al. [8] and Andreeva et al. [16] reported the lowest temperature H_2 TPR peak over their Au/CeO_2 prepared by deposition–precipitation at 150 °C. In addition, there is ample of evidence in the literature to suggest that Au facilities reduction of surface oxygen in ceria at significantly lower temperature than noble metals [8,13] rendering higher activity at the low temperature regime. Our Au–Pt and Au–Pd seem to further enhance the low temperature WGS activity. From curiosity point of view, perhaps one key question is: what is the role(s) of metal particles on ceria in promoting a high activity for WGS at lower temperatures?

With regard to the mechanism there are numerous inconsistencies in the literature. One school of thought is that the WGS reaction over gold–ceria catalysts is involved with a support-mediated surface redox process as shown in Scheme 1 [17]. The adsorbed CO on the metal promoter reacts with ceria to generate cerous oxide and CO_2, with H_2O replenishing the oxygen vacancy with liberation of H_2. But yet there is no evidence for Au–CO interaction identified in gold–ceria catalysts. In addition, Sakurai et al. have recently showed from their CO and water pulse experiments that CO_2 and H_2 were formed at the same time when H_2O was added [13]. That result cannot be accounted by the above 'redox mechanism' for the catalytic behaviour of gold containing ceria catalysts.

Another school of thought is the involvement of surface formate [18]. In this mechanism (see Scheme 2), surface germinal OH groups are thought to act as active sites to form the surface formate intermediate from the reaction with CO, which are generated from the hydrolysis of a partial reduced ceria surface. The decomposition of surface formate (via unidentate carbonate) with water will release CO_2 and H_2. This is supported by spectro-

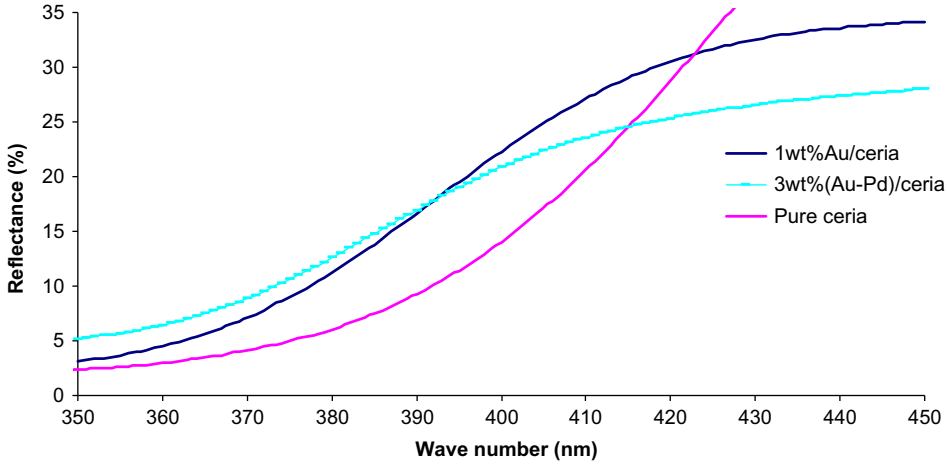

Fig. 4. Typical UV–visible diffuse reflectance spectra of CeO_2, gold doped CeO_2 and 3 wt% (Au–Pd) doped CeO_2 which clearly show the significant shifts in absorption edge of the ceria (O_{2p}–Ce_{4f}) upon doing with metal promoters.

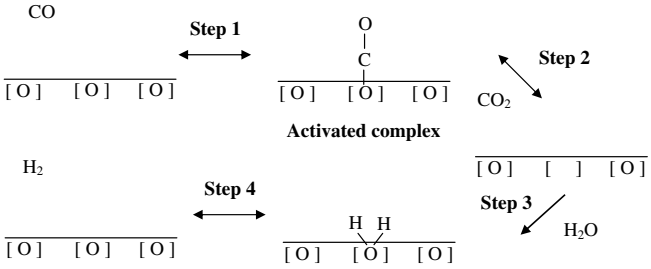

Scheme 1. Proposed redox pathways for WGS reaction over metal promoted ceria.

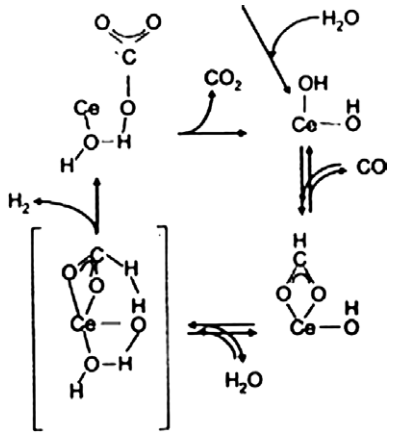

Scheme 2. Bidentate formate mechanism proposed by Shido and Iwasawa [18].

scopic evidence on the existences of germinal hydroxyl groups and formate [19] on ceria surface. According to Davies and co-workers from their detailed DRIFTS and kinetic studies over Au/CeO_2 the 'formate mechanism' is concluded [20]. On the other hand, the transient FTIR results of the Belfast group who questioned the formate as the key intermediate [21]. So far, our result does not allow us to differentiate the 'formate' route from 'redox' mechanism.

In addition, the role of metal promoter is also not clear. It has been proposed that the metal assists reduction of ceria surface at low temperature by hydrogen spillover [22]. However, it is long known that noble metals show high activity than gold in hydrogen spillover. The observation of higher activity of gold containing ceria catalysts in WGS at particularly low temperatures does not seem to endorse this proposal. On the other hand, ceria is a semiconductive oxide the redox properties of which can be altered by doping with foreign promoter. Thus, the electronic band transitions of the ceria samples were evaluated by UV/vis diffuse reflectance (see Table 2). From our diffuse UV–visible reflectance study we clearly observed that there was a significant enlargement in band structure of ceria (a clear blue shift of the absorption edge of O_{2p}–Ce_{4f}) of the n-type semiconducting ceria upon doping with metal promoters). It is therefore proposed that the presence of metal promoter alters the local electronic band structure of ceria facilitating the reduction of surface oxygen. It is noted an electron transfer mechanism could take place at the interface between ceria and metal (with a higher work function) in facilitating the reduction of the ceria [10] as the following $2\,M + 2[O] = 2\,M^{+} + 2[\,] + O_2 + 2\,e^{-}$ [ ]. According to our measurement Au–Pt promoter created the highest band enlargement which matched with the highest WGS activity recorded. Thus, we propose that Au–Pt particles could exert desirable electronic effect (induce the blue shift) on the underneath ceria, creating more active redox sites for the WGS reaction. It should be noted that our TPR results indeed reflected that the significant enhancement in redox properties of ceria by Au–Pt (facilitating the reduction of surface oxygen of ceria at the lowest temperature).

5. Conclusion

From this work, it is found a strong correlation between WGS activity and surface oxygen reducibility of promoted

ceria. This suggests that the partial reduction of ceria is necessary for generating active sites for low temperature WGS reaction. This study also represents the first study on bimetallic gold promotion on ceria for WGS reaction and we also report the high activity of gold–platinum on ceria for the low temperature WGS reaction. Finally, it is proposed (that) the role of the gold containing promoter is to alter the local band structure of ceria facilitating its redox properties at low temperature.

Acknowledgement

MAHJ is grateful to the co-funding from University of Reading and Johnson Matthey towards her PhD degree. Assistances in the BET and EDX measurements by Mr. C.H. Yu of Reading University are kindly acknowledged.

References

[1] X. Qi, M. Flytzani-Stephanopoulos, Ind. Eng. Chem. Res. 43 (2004) 3055.
[2] A. Faur-Ghenciu, The Magazine of Fuel Cell Business and Technology, April/May, 2003.
[3] M.V. Twigg, in: Catalyst Handbook, second ed., Wolfe Publishing, England, 1989.
[4] A. Luengnaruemitchai, S. Osuwan, E. Gulari, Catal. Commun. 4 (2003) 215.
[5] T. Bunluesin, H. Cordados, R.J. Gorte, J. Catal. 157 (1995) 222.
[6] T. Bunluesin, R.J. Gorte, Appl. Catal. B 15 (1998) 107.
[7] M. Haruta, M. Daté, Appl. Catal. A 222 (2001) 427.
[8] Q. Fu, A. Weber, M. Flytzani-Stephanopoulos, Catal. Lett. 77 (2001) 87.
[9] T. Tabakova, F. Boccuzzi, M. Manzoli, J.W. Sobczak, V. Idakiev, D. Andreeva, Appl. Catal. B 49 (2004) 73.
[10] R.R. Rajaram, J.W. Hayes, G.P. Ansell, and H.A. Hatcher, US patent 5,993,762, filed on 30 November, 1999.
[11] G. Liu, J.A. Rodriguez, J. Hrbek, J. Dvorak, J. Phys. Chem. B 105 (2001) 7762.
[12] F. Zamar, A. Trovarelli, C. Leitenburg, G. Dolcetti, J. Chem. Soc., Chem. Commun. (1995) 965.
[13] H. Sakurai, T. Akita, S. Tsubota, M. Kiuchi, M. Haruta, Appl. Catal. A 291 (2005) 179.
[14] A. Venugopal, J. Aluha, M.S. Scurrell, Catal. Lett. 90 (2003) 1.
[15] S. Hilaire, X. Wang, T. Luo, R.J. Gorte, J. Wagner, Appl. Catal. A 215 (2001) 271.
[16] D. Andreeva, Gold Bull. 35 (2002) 82.
[17] C. Rhodes, G.J. Hutchings, A.M. Ward, Catal. Today 23 (1995) 43.
[18] T. Shido, Y. Iwasawa, J. Catal. 141 (1993) 71.
[19] T. Tabakova, F. Boccuzzi, M. Manzoli, D. Andreeva, Appl. Catal. A 252 (2003) 385.
[20] G. Jacobs, E. Chenu, P.M. Patterson, L. Williams, D. Sparks, G. Thomas, B.H. Davis, Appl. Catal. A 258 (2004) 203.
[21] D. Tibiletti, A. Goguet, F.C. Meunier, J.P. Breen, R. Burch, Chem. Commun. (2004) 1836.
[22] G. Jacobs, S. Ricote, P.M. Patterson, U.M. Graham, A. Dozier, S. Khalid, E. Rhodus, B.H. Davis, Appl. Catal. A 292 (2005) 229.